INSTITUTE OF PHYSICS PUBLISHING JOURNAL OF PHYSICS: CONDENSED MATTER

J. Phys.: Condens. Matter **16** (2004) 1613–1621 PII: S0953-8984(04)70087-9

Fano-like resonances in three-quantum-dot Aharonov–Bohm rings

I Gómez[1,3], **F Domínguez-Adame**[1] **and P Orellana**[2]

[1] GISC, Departamento de Física de Materiales, Universidad Complutense, E-28040 Madrid, Spain
[2] Departamento de Física, Universidad Católica del Norte, Casilla 1280, Antofagasta, Chile

E-mail: igcuesta@valbuena.fis.ucm.es

Received 25 September 2003
Published 20 February 2004
Online at stacks.iop.org/JPhysCM/16/1613 (DOI: 10.1088/0953-8984/16/9/009)

Abstract

In this work we study electron transport through quantum wires coupled to a quantum dot Aharonov–Bohm ring by using a noninteracting Anderson tunnelling Hamiltonian. In the case of an asymmetric coupling and three dots within the Aharonov–Bohm ring we have observed the appearance of Fano-like resonances in the conductance. We have investigated the asymmetry and the position of the conductance resonances and found closed expressions. We have also observed Aharonov–Bohm oscillations. Finally the local density of states as well as the probability amplitude phases have been studied.

1. Introduction

Since Fano proposed in 1961 a theoretical framework for explaining the shape of some He resonances observed in electron scattering experiments [1], a large variety of systems [2–5] have shown what seems to be a ubiquitous phenomenon that fits into the framework of the Fano effect. Since then, both experimental [6, 7] and theoretical works [8–10] have been devoted to studying this effect. In particularly, Aharonov–Bohm interferometers with embedded quantum dots have received notable attention in the last few years. These works considered the asymmetric Fano lineshapes observed in the conductance of these mesoscopic systems [9–11], as well as quantum coherence phenomena such as the Kondo effect [12, 13]. The observed Fano lineshapes arise from the quantum mechanical interference between the quantum dot resonant state and the continuum [1]. Also, as regards these quantum dot Aharonov–Bohm interferometers, a number of papers have been devoted to analysing phase and coherence properties [6, 8, 7, 14].

In this paper we study electron transport through quantum wires coupled to a quantum dot Aharonov–Bohm ring. The ring is formed by N quantum dots which are connected to

[3] Author to whom any correspondence should be addressed.

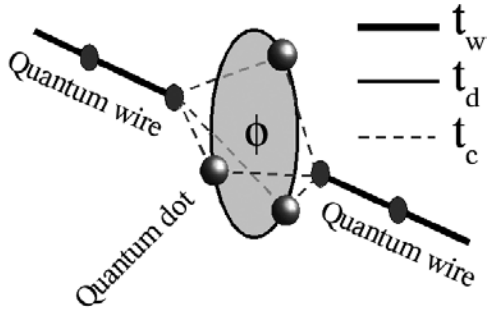

Figure 1. A schematic diagram of the quantum dot Aharonov–Bohm ring. See the text for further details.

each other by a coupling constant t_d. Besides this, the dots belonging to the ring are coupled to two quantum wires via a coupling constant t_c. The wires act as contacts so it is possible to establish a current through the ring. In addition, a magnetic field is applied and a magnetic flux Φ is then established through the ring.

This paper is organized as follows. First, in section 2 we briefly describe the formalism used to study this system. We present closed expressions for the conductance when a magnetic field is applied, and find Aharonov–Bohm oscillations. In section 3 we particularize to the simplest case $N = 3$ and find that an asymmetry of the ring coupling constant induces the appearance of Fano-like resonances. We give closed expressions for the resonant and antiresonant energies of the Fano-like conductance resonances appearing and study how their position and lineshape depend on the different system parameters. For an applied magnetic field, as in the symmetric case, we observe Aharonov–Bohm conductance oscillations. In section 4 we investigate the local density of states at the dots belonging to the Aharonov–Bohm ring, and the phase jumps taking place at the antiresonant energy. Finally, section 5 concludes the paper with a summary of results and a discussion on their relevance in describing actual experiments.

2. Model

We model the system described previously by using a noninteracting Anderson tunnelling Hamiltonian that can be written as $\mathcal{H} = \mathcal{H}_W + \mathcal{H}_R^N + \mathcal{H}_{WR}^N$, where

$$\begin{aligned}
\mathcal{H}_W &= \varepsilon_0 \sum_j c_j^\dagger c_j + t_w \sum_j (c_j^\dagger c_{j+1} + c_{j+1}^\dagger c_j), \\
\mathcal{H}_R^N &= \varepsilon \sum_{i=1}^N d_i^\dagger d_i + t_d \sum_{i=1}^N (e^{i\phi} d_i^\dagger d_{i+1} + e^{-i\phi} d_{i+1}^\dagger d_i), \\
\mathcal{H}_{WR}^N &= t_c \sum_{i=1}^N (d_i^\dagger c_1 + c_1^\dagger d_i + d_i^\dagger c_{-1} + c_{-1}^\dagger d_i),
\end{aligned} \tag{1}$$

where ε is the site energy at the quantum dots. Here ϕ is the Peierls phase: $\phi = 2\pi\Phi/N\Phi_0$, where $\Phi_0 = h/e$ is the flux quantum. The operators $c_j^\dagger$, $d_i^\dagger$ (c_j, d_i) create (annihilate) an electron at sites j (wires) and i (ring), respectively. Hereafter we will assume a coupling constant equal to unity ($t_w = 1$) and zero site energy in the wires ($\varepsilon_0 = 0$) without loss of generality. A schematic view of the device is depicted in figure 1.

The stationary states of the entire Hamiltonian $\mathcal{H}$ can be written as

$$|\psi\rangle = \sum_j a_j|j\rangle + \sum_i b_i|i\rangle, \tag{2}$$

where the coefficient a_j (b_i) is the probability amplitude for finding the electron at site j of the wires (i of the ring). From (1) and (2), the equations for the Wannier amplitudes a_j and b_i on the wires and the ring respectively can be written in the following way:

$$\begin{aligned} Ea_j &= a_{j-1} + a_{j+1}, \\ Ea_{-1} &= a_{-2} + t_c \sum_{i=1}^{N} b_i, \\ Ea_1 &= a_2 + t_c \sum_{i=1}^{N} b_i, \\ Eb_i &= t_d(e^{i\phi} b_{i+1} + e^{-i\phi} b_{i-1}) + \varepsilon b_i + t_c(a_1 + a_{-1}), \end{aligned} \tag{3}$$

with $i = 1, 2, \ldots, N$ and $j = \pm 2, \pm 3, \ldots$. In what follows we will restrict ourselves to the study of the zero-temperature conductance. For a single electron channel we have

$$G = \frac{2e^2}{h}\tau, \tag{4}$$

where τ is the transmission coefficient. In order to calculate τ we assume that the electrons are described by a plane wave incident from, say, the left wire ($j < -1$) with unity amplitude and a reflected wave with reflection amplitude r. At the right wire ($j > 1$) electrons are described by a transmission amplitude t. Taking this to be the solution of equation (3) at the wires, the transmission coefficient can be written as $\tau = |t|^2$. Introducing the following notation:

$$\Gamma_N \equiv 2Nt_c^2, \qquad \Omega \equiv 2t_d \cos\phi, \tag{5}$$

and performing some lengthy algebra we arrive at the expression for the zero-temperature electron conductance:

$$G(N, \Phi) = \frac{(2e^2/h)\Gamma_N^2(1 - E^2/4)}{\Gamma_N^2 + (\varepsilon - E + \Omega)^2 + E\Gamma_N(\varepsilon - E + \Omega)}. \tag{6}$$

From this expression we conclude that the conductance presents resonant energies given by

$$E_\uparrow = \frac{\varepsilon + \Omega}{1 - \Gamma_N/2}, \qquad E_\downarrow = 4\frac{1 - \Gamma_N/2}{\varepsilon + \Omega}. \tag{7}$$

These two energies cannot lie simultaneously within the wire band since they satisfy the relation $4 = E_\uparrow E_\downarrow$. From (6) and (7) it can be observed that the resonant energies depend on the different system parameters. The width depends on the coupling between the wires and the ring t_c and the system size N. It is clear that the resonant peak broadens as the system size increases.

Aharonov–Bohm oscillations can be observed in this system as the conductance depends on the oscillatory term Ω, due to the presence of the ring-enclosed magnetic flux Φ. Figure 2 shows the conductance as a function of the magnetic flux Φ when the Fermi energy is located at the band centre $E = \varepsilon = 0$, with $t_c = 0.1$ and $t_d = 0.5$. For this energy it can be seen from expression (7) that the conductance reaches its maximum ($2e^2/h$) when the magnetic flux satisfies $\Phi/N\Phi_0 = (2n + 1)/4$, $n = 0, 1, 2, \ldots$.

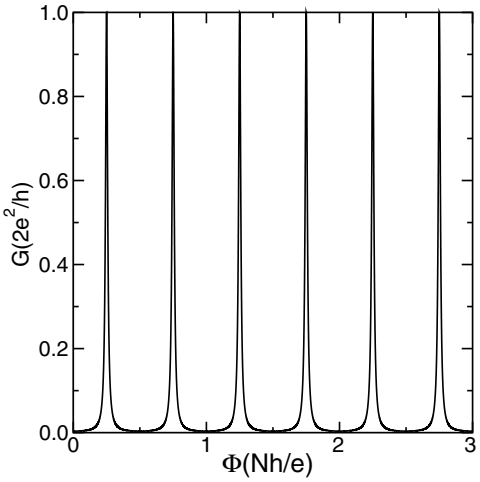

Figure 2. The conductance as a function of the magnetic flux. Aharonov–Bohm oscillations can be observed.

3. Fano-like resonances

Now we particularize our results to the case with only three quantum dots in the ring, $N = 3$. Besides this, we consider a single defect (asymmetric Aharonov–Bohm ring) in the ring, which consists in a coupling constant between two of the three dots differing from the two others by a factor α: $\bar{t}_\mathrm{d} = \alpha t_\mathrm{d}$. In our present calculations we will assume that $\varepsilon = 0$ for all the dots belonging to the ring.

As we did in the general case, it is possible to calculate the conductance arriving at the following expression:

$$G(N = 3, \Phi) = \frac{(2e^2/h)\Gamma(E, \Phi)^2(1 - E^2/4)}{\Gamma(E, \Phi)^2 + \Omega(E, \Phi)^2 + E\Gamma(E, \Phi)\Omega(E, \Phi)}. \tag{8}$$

The form of this equation resembles that of (6) but now, due to the presence of the defect $\bar{t}_\mathrm{d}$ in the asymmetric ring, the quantities Γ and Ω are much more complex and involve both E and Φ. Here

$$\Gamma(E, \Phi) = 2t_\mathrm{c}^2\gamma(E, \Phi)^2,$$

with

$$\gamma(E, \Phi) = 3E^2 + 2(2 + \alpha)t_\mathrm{d}E\cos\phi + t_\mathrm{d}^2[4(1 + 2\alpha)\cos^2\phi - (\alpha + 2)^2],$$

and

$$\Omega(E, \Phi) = E^3 - (2 + \alpha^2)Et_\mathrm{d}^2 + 2\alpha t_\mathrm{d}^3\cos\phi[3 - 4\cos^2\phi].$$

It is possible to find a set of system parameters for which the conductance presents an antiresonance. This will happen for an energy satisfying $\gamma(E, \Phi) = 0$. The conductance will also show a resonance when the condition $E\gamma(E, \phi)t_\mathrm{c}^2 = \Omega(E, \Phi)$ is fulfilled. Particularizing to the case in which $\Phi/3\Phi_0 = 1/4$, that is $\cos\phi = 0$, we obtain

$$E_\mathrm{r} = \pm t_\mathrm{d}\sqrt{\frac{2 + \alpha^2 - t_\mathrm{c}(2 + \alpha)^2}{1 - 3t_\mathrm{c}}}, \qquad E_\mathrm{r} = 0, \tag{9a}$$

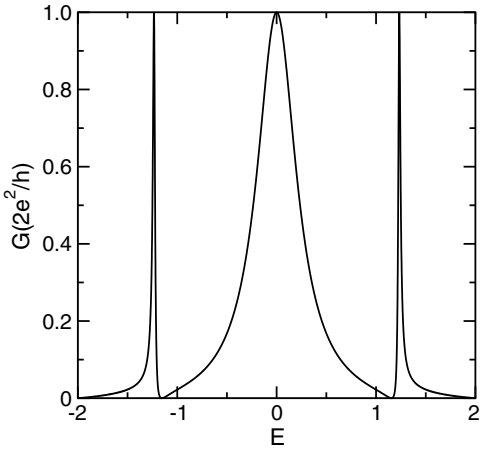

Figure 3. The conductance as a function of the Fermi energy in a three-quantum-dot Aharonov–Bohm ring.

and

$$E_{\mathrm{a}} = \pm t_{\mathrm{d}} \frac{2+\alpha}{\sqrt{3}}, \tag{9b}$$

for the resonant and antiresonant energies respectively. From these equations it is clear that the energy of the resonances changes with the asymmetry parameter as $E \sim \alpha$. This behaviour seems to be rather general despite the value of the magnetic flux, except for some pathological cases, such as $t_{\mathrm{c}} = 1$ and $\Phi/3\Phi_0 = 1/4$; then $E_{\mathrm{a}} \sim \alpha$ and $E_{\mathrm{r}} \sim \sqrt{\alpha}$. In figure 3 we plot the conductance as a function of the Fermi level in units of the coupling constant within the wires for $t_{\mathrm{d}} = 1/2$, $\alpha = 2$ and $t_{\mathrm{c}} = 0.2$. One can see the appearance of two symmetrically located Fano-like resonances with a characteristic asymmetric lineshape at the energies given by equation (9*a*). As previously stated, Fano resonances arise whenever a quantum interference between a resonant state and a continuum takes place [1]. In the present case the Fano-like lineshapes shown in figure 3 can be understood as an interference between the different paths (a consequence of the asymmetry α in the coupling constant connecting the dots in the ring) that connect the left and the right wires of the system. Note the occurrence of a resonant energy at $E = 0$ that is reminiscent of the symmetric case ($\alpha = 1$).

The Fano-like resonances found appear not only for nonzero magnetic flux. In a general case the expressions for the resonant and antiresonant energies are more complicated, but it is still possible to find closed expressions for these quantities. In figure 4 we represent the conductance versus the Fermi energy for zero magnetic flux. The system parameters are $\Phi/3\Phi_0 = 0$, $\alpha = 3/2$, $t_{\mathrm{d}} = 1/2$, and (a) $t_{\mathrm{c}} = 0.2$, (b) $t_{\mathrm{c}} = 0.3$, (c) $t_{\mathrm{c}} = 0.5$. The conductance curve is no longer symmetric but still shows a Fano-like resonance. The energy of the resonance changes slightly with the coupling constant t_{c}, but it is worth noting that this parameter controls the asymmetry of the lineshape: the larger t_{c}, the larger the asymmetry, as can be observed in figure 4. It is also remarkable that the present set-up allows tunable Fano-like resonances since both the position and the lineshape can be modified by a suitable selection of the system parameters. Another example of a tunable Fano system has been recently studied experimentally [7, 15].

Figure 5 shows the conductance as a function of the magnetic flux (in units of the flux quantum) when the Fermi energy is located at the centre of the band ($E = \varepsilon = 0$), of a

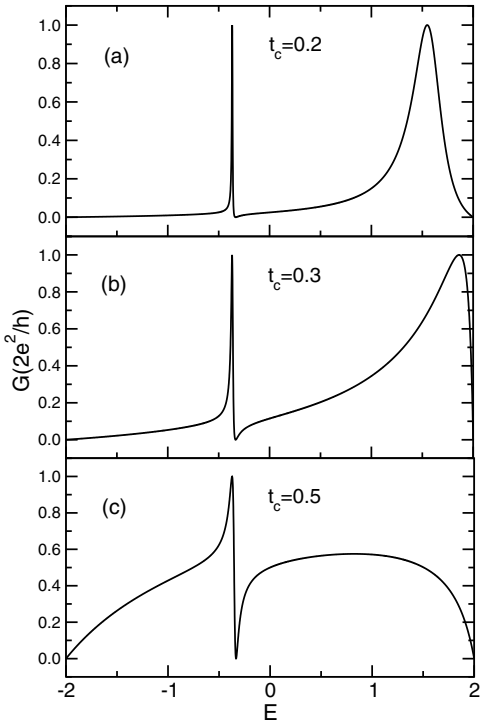

Figure 4. The conductance as a function of the Fermi energy in the three-quantum-dot Aharonov–Bohm ring showing the lineshape dependence on the coupling t_c.

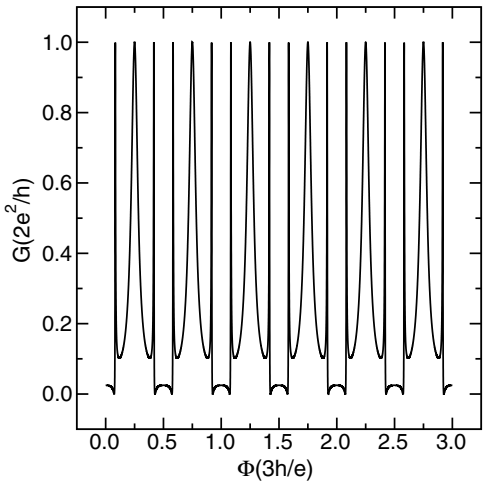

Figure 5. The conductance as a function of the magnetic flux in the three-quantum-dot Aharonov–Bohm ring.

three-quantum-dot Aharonov–Bohm ring. In the figure, $t_c = 0.2$, $t_d = 1/2$ and $\alpha = 2$. From equation (8) and figure 5 it is clear that the asymmetry α does not affect the presence of conductance oscillations due to the oscillatory term $\cos\phi$. These oscillations present several

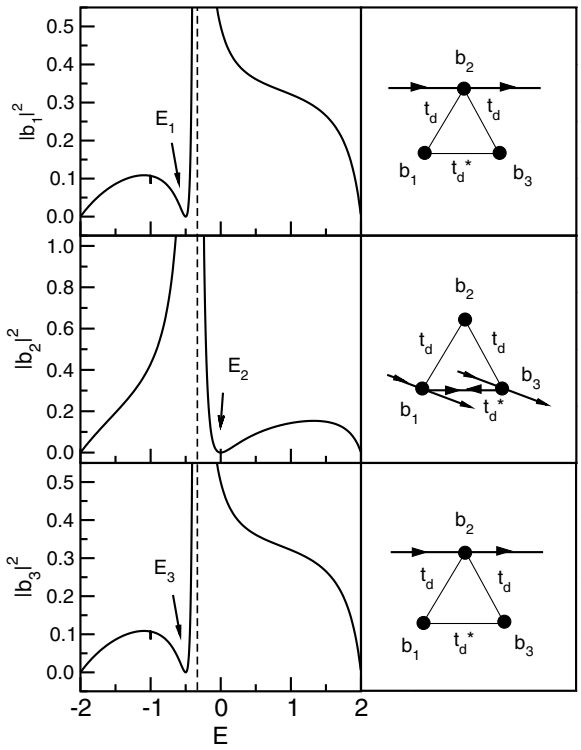

Figure 6. The local density of states as a function of the Fermi energy for each quantum dot belonging to the ring. We show schematically the electronic open paths for the energies marked with an arrow. The dashed line indicates the antiresonant energy.

maxima, six for each period, two of them for values of the flux given by $\Phi/3\Phi_0 = (2n+1)/4$, $n = 0, 1, 2, \ldots$, which are reminiscent of those in the symmetric ($\alpha = 1$) case. The other maxima are associated with the already mentioned symmetric Fano-like resonances.

4. Local density of states and phase jumps

It is not difficult to find from (3) the local density of states at each quantum dot belonging to the ring, which will allow us to better understand the observed Fano-like resonances. We study the case with vanishing magnetic flux ($\Phi = 0$). After some algebra we arrive at the following expressions:

$$|b_1|^2 = |b_3|^2 = \frac{(4-E^2)(E+t_d)^2 t_c^2}{\delta^2+\beta^2}, \qquad |b_2|^2 = \frac{(4-E^2)[E-(\alpha-2)t_d]^2 t_c^2}{\delta^2+\beta^2}, \tag{10a}$$

where

$$\delta = E^2 - \alpha t_d E - 2t_d^2, \qquad \beta = (6E - 2\alpha t_d + 8)t_c^2. \tag{10b}$$

In figure 6 we plot the local density of states using the same parameters as in figure 4(c) for the three quantum dots belonging to the ring. It can be seen that the three curves present a resonance for an energy equal to the conductance resonant energy. Thus the dots are maximally charged

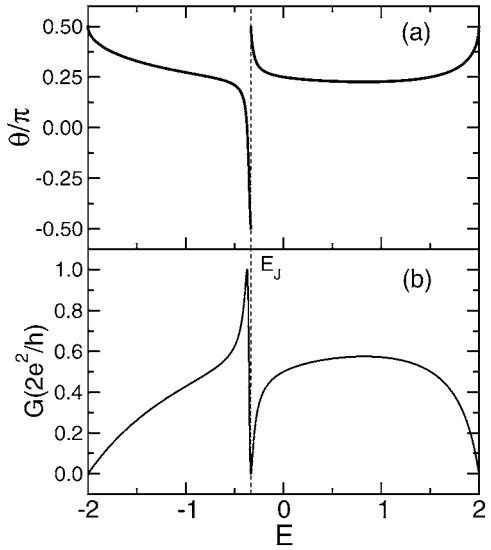

Figure 7. (a) The probability amplitude phase, and (b) the conductance as a function of the Fermi energy. The dashed line indicates the antiresonant energy.

at this resonant energy. One might naively expect the dots to be empty at the conductance antiresonant energy. However, the dots are charged. This supports the idea that the origin of this antiresonance is the interference between the different paths in the ring. If one calculates the antiresonant energy for the present case, which turns out to be $E_a = t_d(\alpha - 4)/4$, it can be found that $|b_2|^2/|b_1|^2 = 4$ for this energy, which is highly surprising since it becomes independent of any system parameter. It can be observed in figure 6 that there exist some energies that do not correspond to the antiresonant energy for which the local density of states becomes zero, namely $|b_1|^2 = |b_3|^2 = 0$ or $|b_2|^2 = 0$. At these energies

$$E_1 = E_3 = -t_d, \qquad E_2 = (\alpha - 2)t_d, \tag{11}$$

marked in the figure with an arrow, some of the interfering paths are closed and the electron transport takes place across one or two of the three dots, as is schematically shown on the right-hand side of the figure.

To end our study of the three-quantum-dot Aharonov–Bohm ring we have calculated the phase θ_j for the probability amplitudes, $b_j = |b_j| \exp i\theta_j$ ($j = 1, 2, 3$):

$$\theta_j \equiv \theta = \arctan\left\{\frac{1}{2\sqrt{1 - E^2/4}}\left[\frac{E(\beta - E\delta/2) - 2(1 - E^2/4)\delta}{\beta}\right]\right\}. \tag{12}$$

In figure 7 we show the phase θ for a system with the same parameters as in figure 6. We observe the existence of a phase jump $\Delta\theta = \pi$ at an energy given by the zeros of the denominator in equation (12), $\beta = 0$; that is, $E_J = t_d(\alpha - 4)/3$. This energy corresponds to the antiresonance on the conductance curve. Similar π phase jumps in the transmission amplitudes of Aharonov–Bohm rings with a coupled quantum dot exhibiting the Fano effect have been reported both experimentally [6, 16] and theoretically [8, 14, 17, 18]. The origin of these phase jumps in these systems has been attributed to a coupling between the Aharonov–Bohm ring and the quantum dot in these interferometers.

5. Summary

In the present work we have studied electron transport across a quantum dot Aharonov–Bohm ring attached to a pair of quantum dot wires. We have studied the symmetric N case (all the coupling constants connecting dots within the ring are the same), finding that this system exhibits Aharonov–Bohm oscillations in the conductance. We have also studied the asymmetric case for $N = 3$ in which one of the coupling constants differs from the others by a factor α. We have observed in this case the appearance of Fano-like resonances. The system can be tuned by varying the system parameters, since both the position and the asymmetry of the resonances can be controlled. In particular, we have found that the asymmetry of the Fano-like resonances is controlled by the constant of coupling, t_c, between the wires and the ring. It has been shown that the asymmetric case still presents Aharonov–Bohm oscillations. We have studied the local density of states on the dots belonging to the ring. The local densities of states found at the dots within the ring show that the observed Fano-like resonances are a consequence of an interference between the different paths across the ring. Finally, we have found a π phase jump in the probability amplitudes similar to those reported in the literature for other quantum dot Aharonov–Bohm interferometers exhibiting the Fano effect.

We expect the above picture to remain valid even if the electron–electron interaction is taken into account. In fact, in embedded quantum dots arrays, the main effect of the electron–electron interaction is to shift and split the resonance positions [19, 20]. This effect arises because the on-site Coulomb repulsion energy U introduces a renormalization of the site energies. From the analogy with embedded quantum dot arrays, we expect that, depending on the relation between the interdot coupling and the on-site Coulomb interaction, different regimes might arise. For U small, the resonances and antiresonances would split into two distinct minibands separated by the on-site Coulomb energy, while for U large, the resonances would occur in pairs.

Acknowledgments

Work at Madrid was supported by DGI-MCyT (Ref. MAT2003-01533). Work at UCN was supported by Milenio ICM P02-054-F and FONDECYT under grants 1020269 and 7020269.

References

[1] Fano U 1961 *Phys. Rev.* **124** 1866
[2] Cerdeira F, Fjeldly T A and Cardona M 1973 *Phys. Rev.* B **8** 4734
[3] Faist J, Capasso F, Sirtori C, West K W and Pfeiffer L N 1997 *Nature* **390** 589
[4] Madhavan V, Chen W, Jamneala T, Crommie M F and Wingreen N S 1998 *Science* **280** 567
[5] Kubala B and König J 2002 *Phys. Rev.* B **65** 245301
[6] Yacobi A, Heiblum M, Mahalu D and Shtrikman H 1995 *Phys. Rev. Lett.* **74** 4047
[7] Kobayashi K, Aikawa H, Katsumoto S and Iye Y 2002 *Phys. Rev. Lett.* **88** 256806
[8] Ryu C and Cho S Y 1998 *Phys. Rev.* B **58** 3572
[9] Kang K 1999 *Phys. Rev.* B **59** 4608
[10] Zeng Z Y, Claro F and Pérez A 2002 *Phys. Rev.* B **65** 085308
[11] Ladrón de Guevara M L, Claro F and Orellana P 2003 *Phys. Rev.* B **67** 195335
[12] Hofstetter W, König J and Schoeller H 2001 *Phys. Rev. Lett.* **87** 156803
[13] Rejec T and Ramšak A 2003 *Preprint* cond-mat/0303258
[14] Aharony A, Entin-Wohlman O, Halperin B I and Imry Y 2002 *Phys. Rev.* B **66** 115311
[15] Kobayashi K, Aikawa H, Katsumoto S and Iye Y 2003 *Physica* E **18** 56
[16] Schuster R, Buks E, Heiblum M, Mahalu D, Umansky V and Shtrikman H 1997 *Nature* **385** 417
[17] Yeyati A L and Büttiker M 1995 *Phys. Rev. Lett.* **76** 110
[18] Yacoby A, Schuster R and Heiblum M 1996 *Phys. Rev.* B **53** 9583
[19] Chen G, Klimeck G, Datta S, Chen G and Goddard W A III 1994 *Phys. Rev.* B **50** 8035
[20] Yu Z, Johnson A T and Heinzel T 1998 *Phys. Rev.* B **58** 13830